

Supporting Information for

Amorphous Array of Poly(*N*-isopropylacrylamide) Brush-Coated Silica Particles for Thermally Tunable Angle-Independent Photonic Band Gap Materials

Yoshie Gotoh,^a Hiromasa Suzuki,^a Naomi Kumano,^a Takahiro Seki,^a Kiyofumi Katagiri,^b and Yukikazu Takeoka^{a*}

^a*Department of Molecular Design & Engineering, Nagoya University, Furo-cho, Chikusa-ku, Nagoya, 464-8603, Japan*

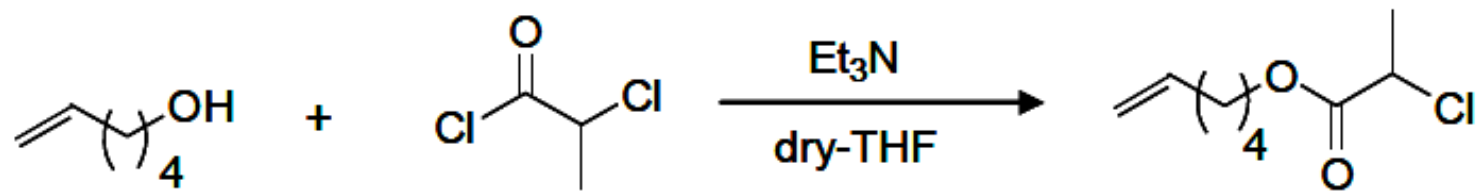
E-mail: ytakeoka@apchem.nagoya-u.ac.jp

^b*Department of Applied Chemistry, Graduate School of Engineering, Nagoya University, Furo-cho, Chikusa-ku, Nagoya 464-8603, Japan*

*To whom correspondence should be addressed. E-mail: ytakeoka@apchem.nagoya-u.ac.jp

Table 1S

Sample No.	[M] : [I] : [Cu ₁] : [L] (M / DMSO) (w/w)	Temperature (°C)	Reaction time (h)	Conversion (%)	$M_{n\text{-theol.}} / 10000$	$M_{n\text{-GPC}} / 10000$	M_w / M_n
1'				81	4.58	3.77	1.26
2'				63	3.56	3.34	1.20
3'				80	4.52	3.80	1.24
4'				70	3.96	3.58	1.21
5'				85	4.80	3.52	1.27
6'				71	4.00	3.49	1.26
7'	500 : 1 : 1 : 1	20	5	80	4.52	2.85	1.20
8'	(1/2)			77	4.35	3.62	1.20
9'				70	3.96	4.42	1.24
10'				65	3.69	4.26	1.32
11'				84	4.75	4.26	1.32
12'				72	4.07	3.74	1.24
13'				92	5.20	4.09	1.27
14'				70	3.96	2.56	1.29
Ave.				76		3.66	1.25



5-hexen-1-yl 2-chloro-2-methylpropionate

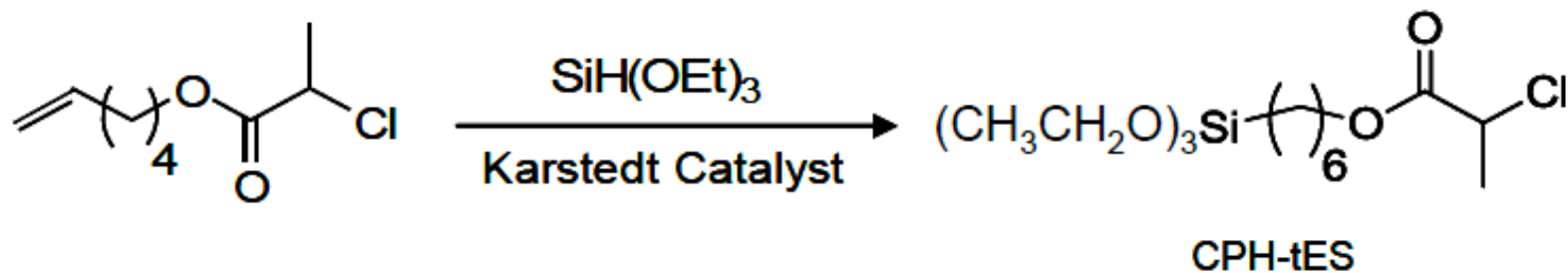


Figure S1. Synthetic route of 6-(2-chloro)propionyloxyhexyltriethoxysilane (CPH-tES).

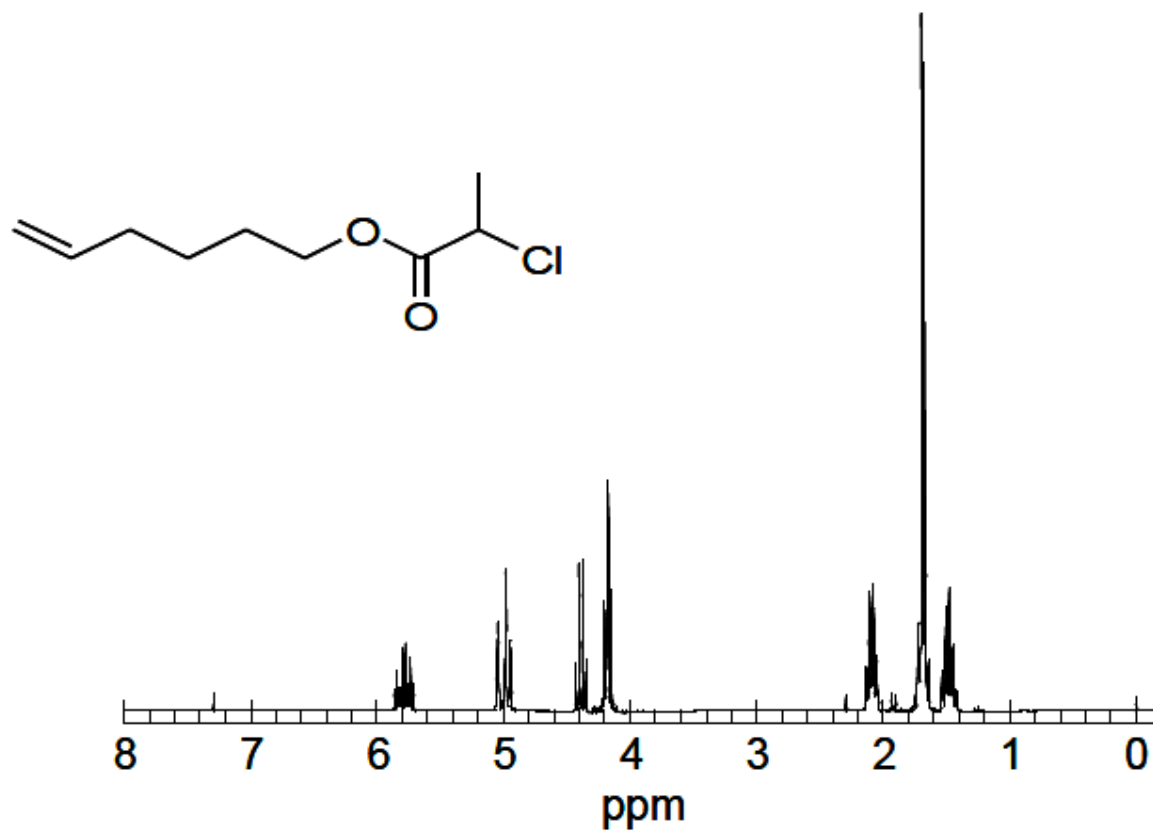


Figure S2. ¹H NMR spectrum of 5-hexen-1-yl 2-chloro-2-methylpropionate in CDCl₃.

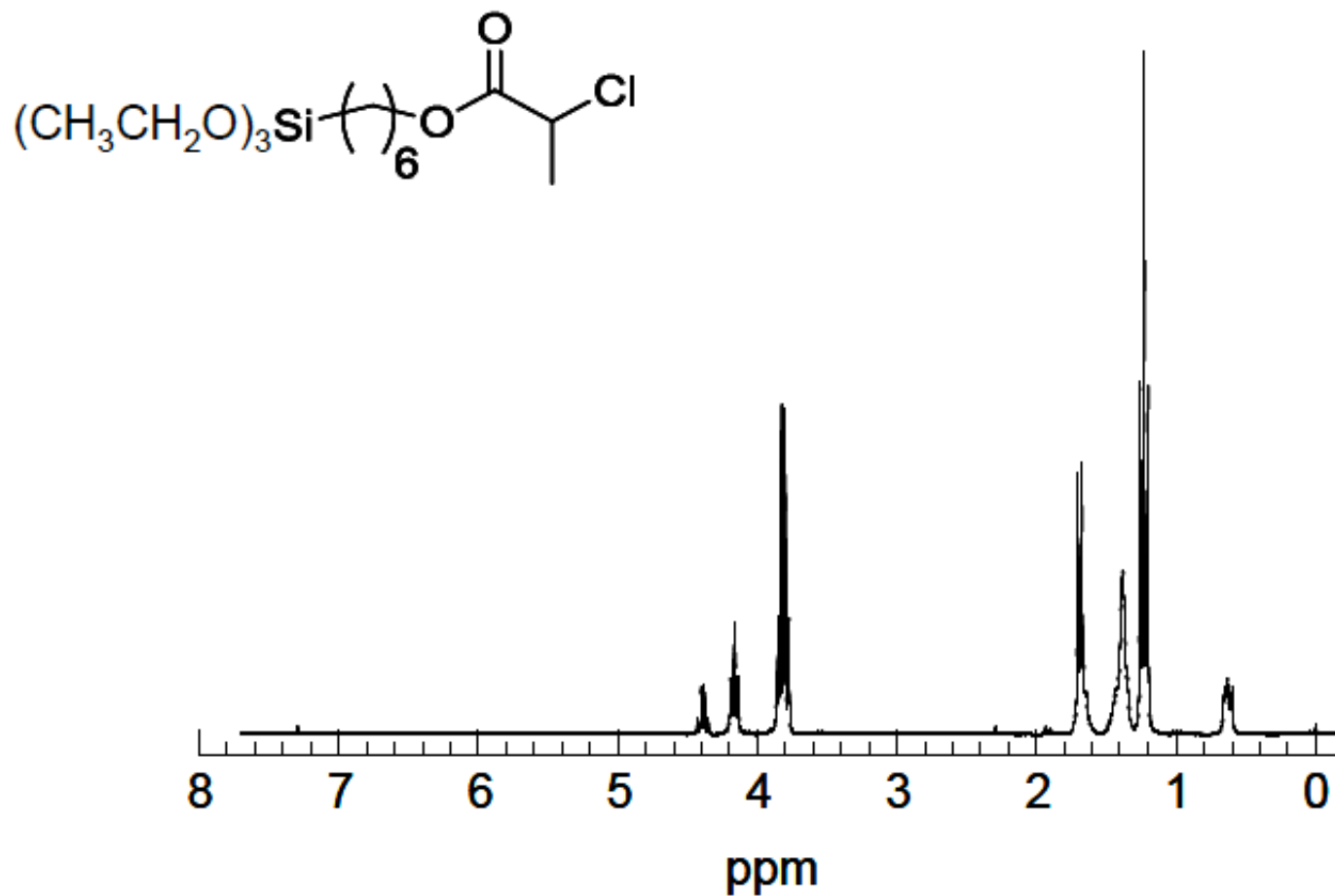


Figure S3. ¹H NMR spectrum of CPH-tES in CDCl_3 .

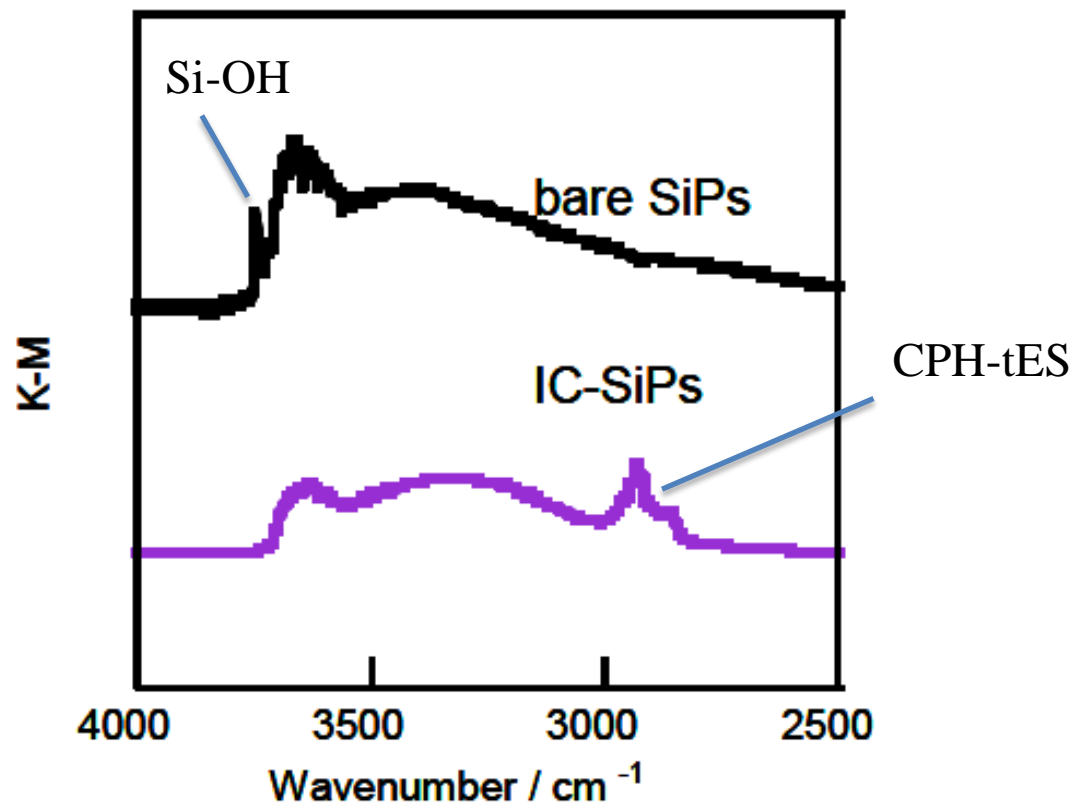


Figure S4. Diffuse reflectance FT-IR spectra of bare SiO₂ particle (bare SiPs) and Initiator Coated SiO₂ particle (IC-SiPs).

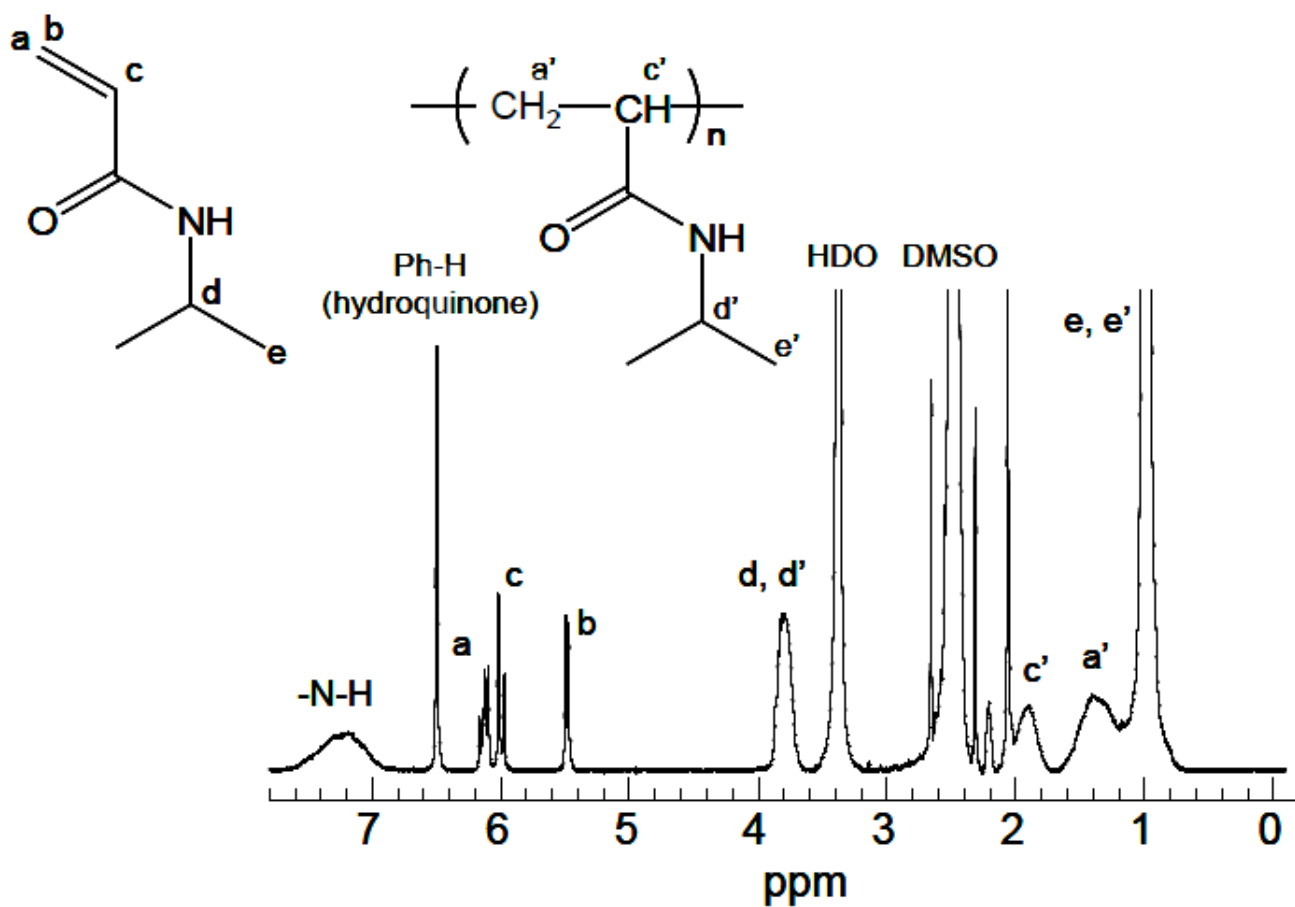


Figure S5. $^1\text{H-NMR}$ spectra of ATRP reaction solution for NIPA before purification in d -DMSO. This data was used to determine the monomer conversion.

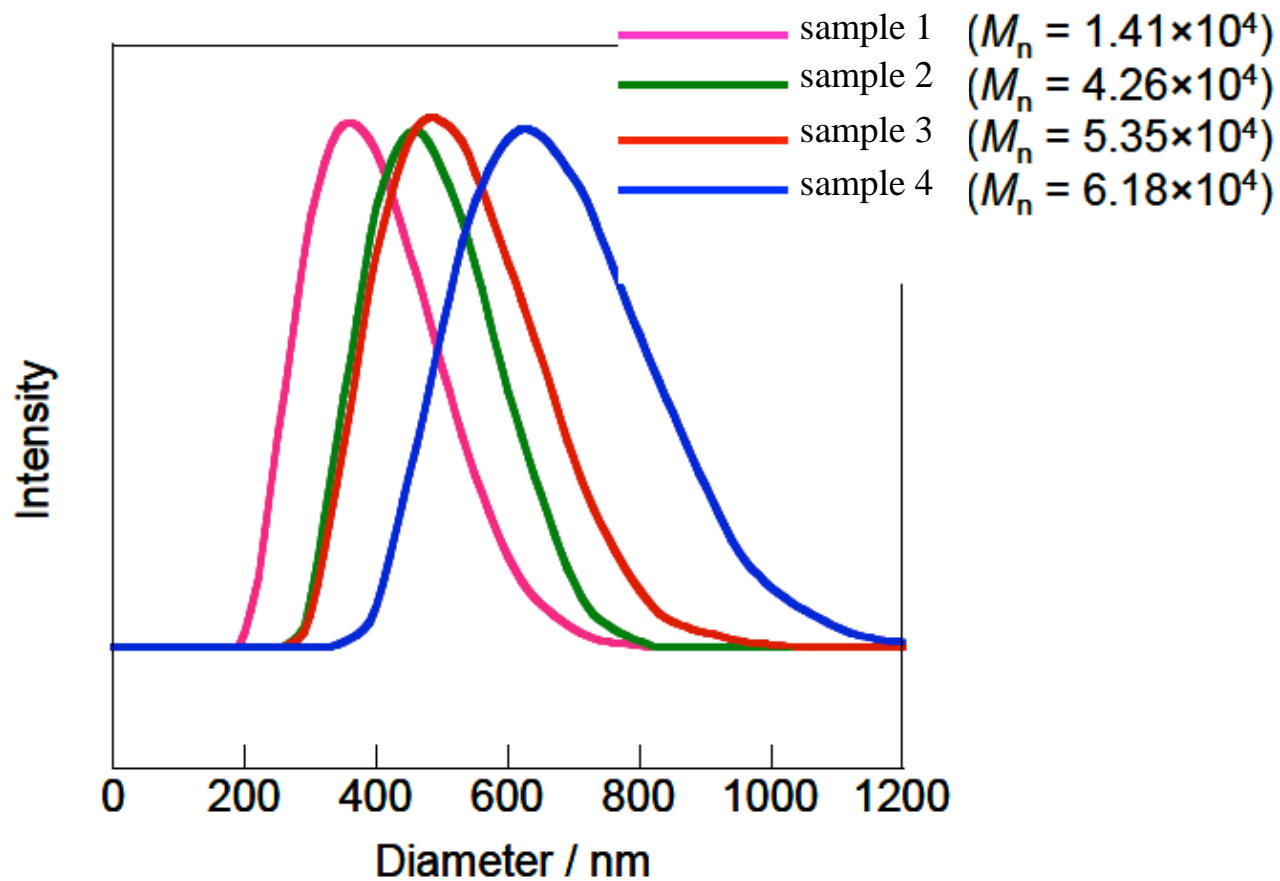


Figure S6. GPC traces for free PNIPA of sample 1-4.

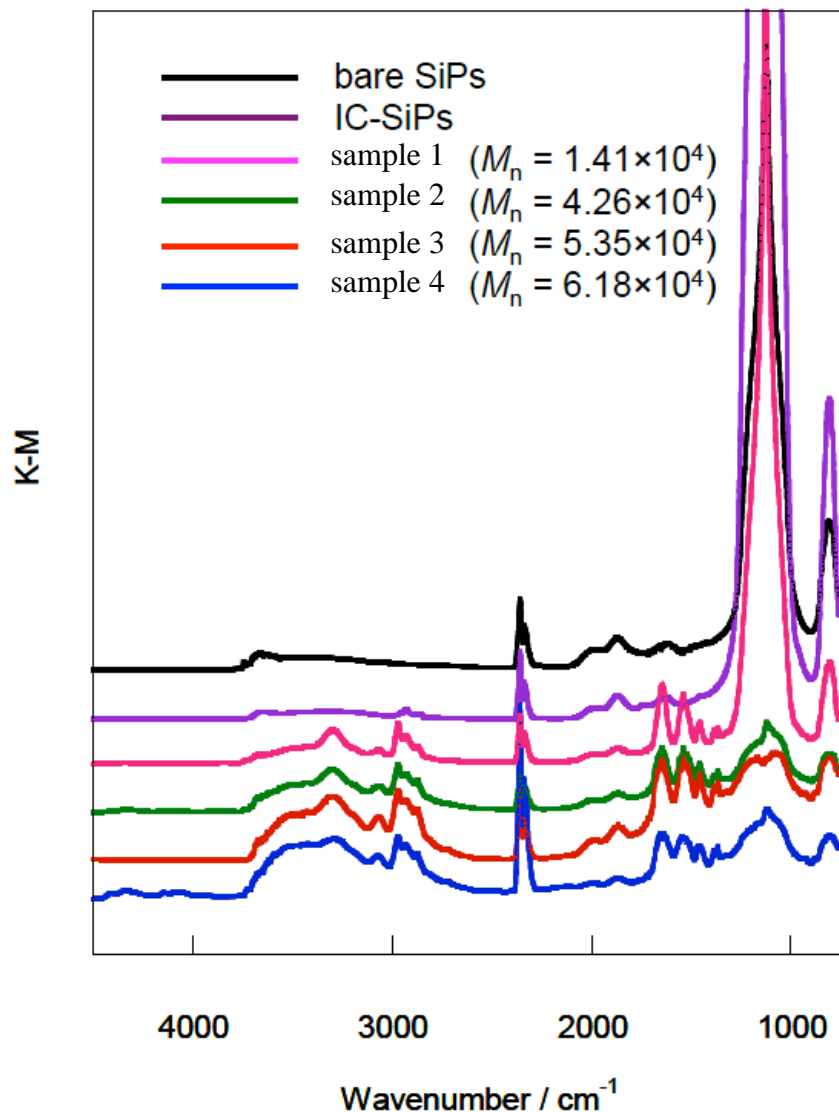


Figure S7. FT-IR spectra of bare SiO₂ particle and PNIPA-SiPs with different polymer chain length. The presence of PNIPA in the resulting particles was confirmed by these diffuse reflectance FT-IR spectra.

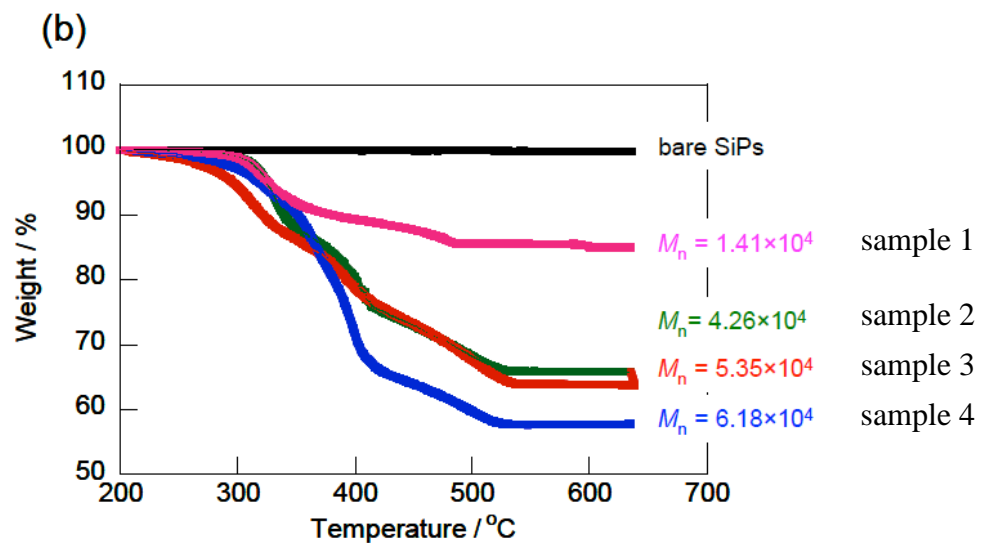
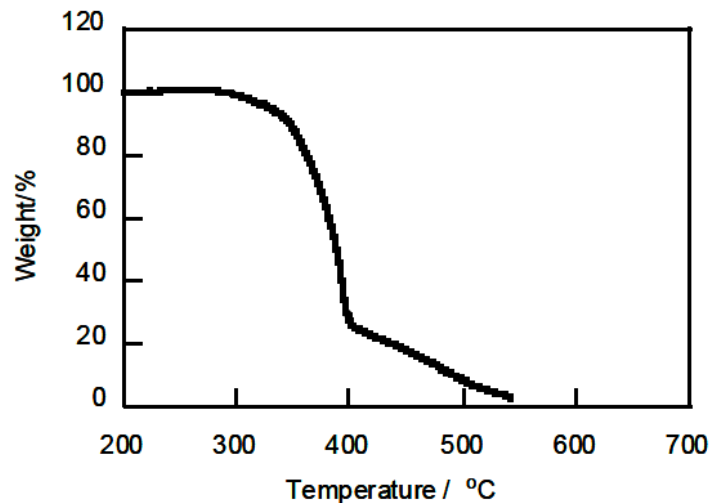
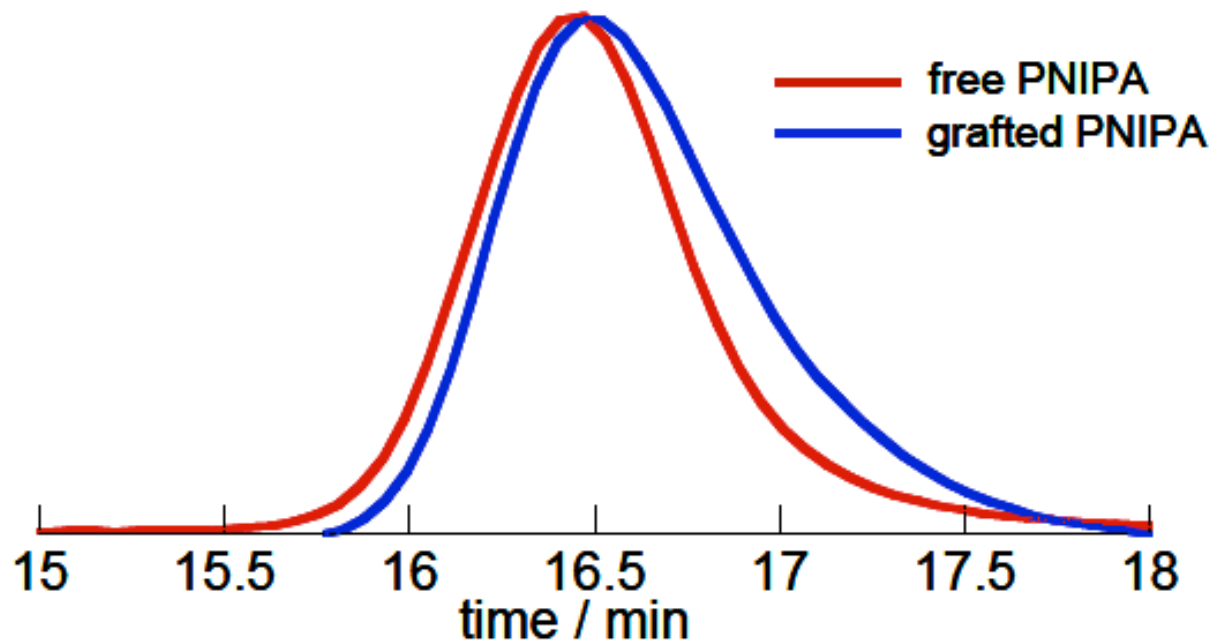


Figure S8. Thermogravimetric Analysis in air: TG of (a) free PNIPA, (b) bare SiO₂ particle and PNIPA-SiPs of sample 1-4.



	$M_n / 10^4$	M_w / M_n
free PNIPA	4.61	1.21
grafted PNIPA	4.10	1.31

Figure S9. GPC chart of free PNIPA and grafted PNIPA.

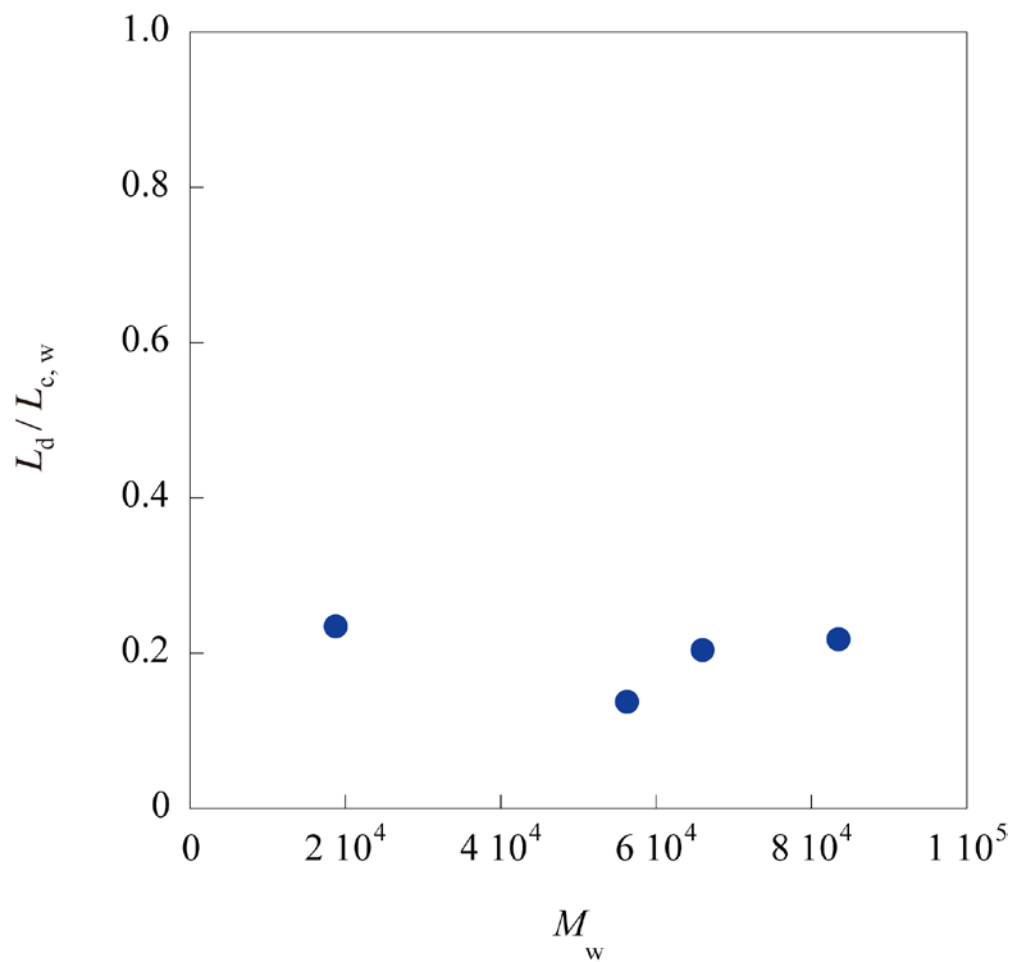


Figure S10. Plots of $L_d/L_{c,w}$ versus weight average molecular weight, M_w .

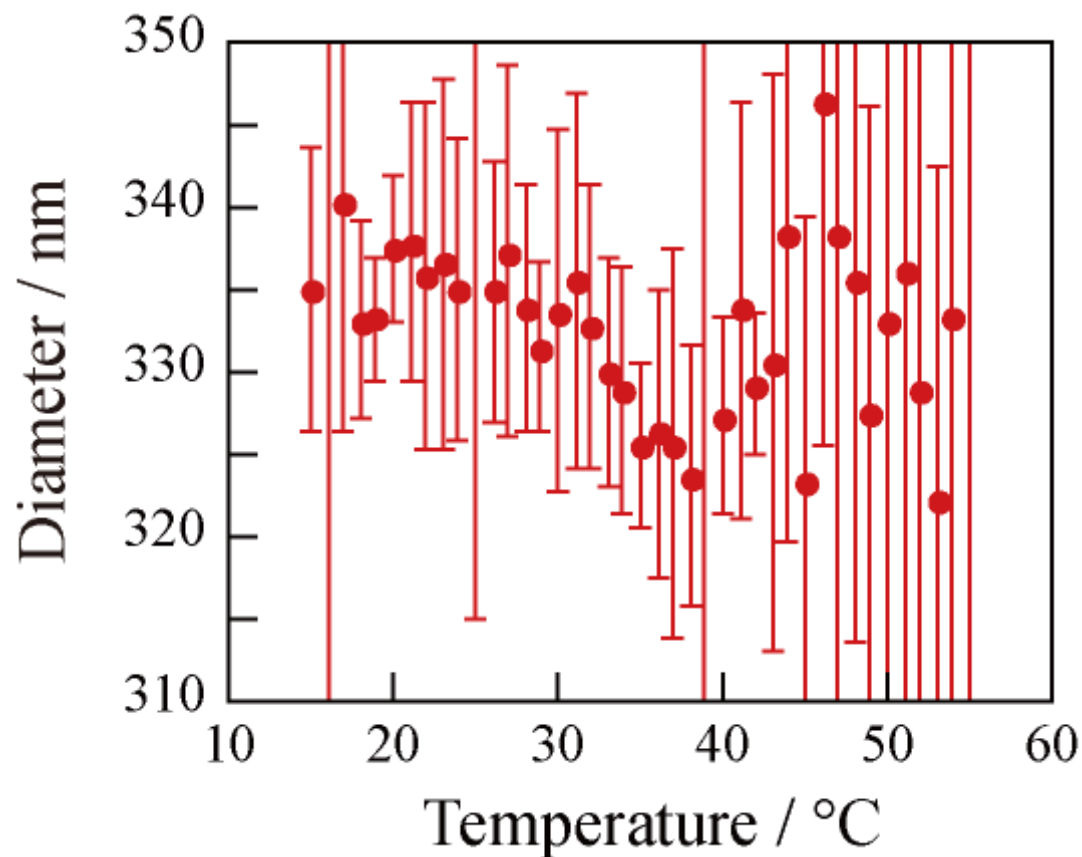


Figure S11. Temperature dependence of the hydrodynamic diameter for PNIPA-SiPs with PNIPA of $M_n = 1.41 \times 10^4$.

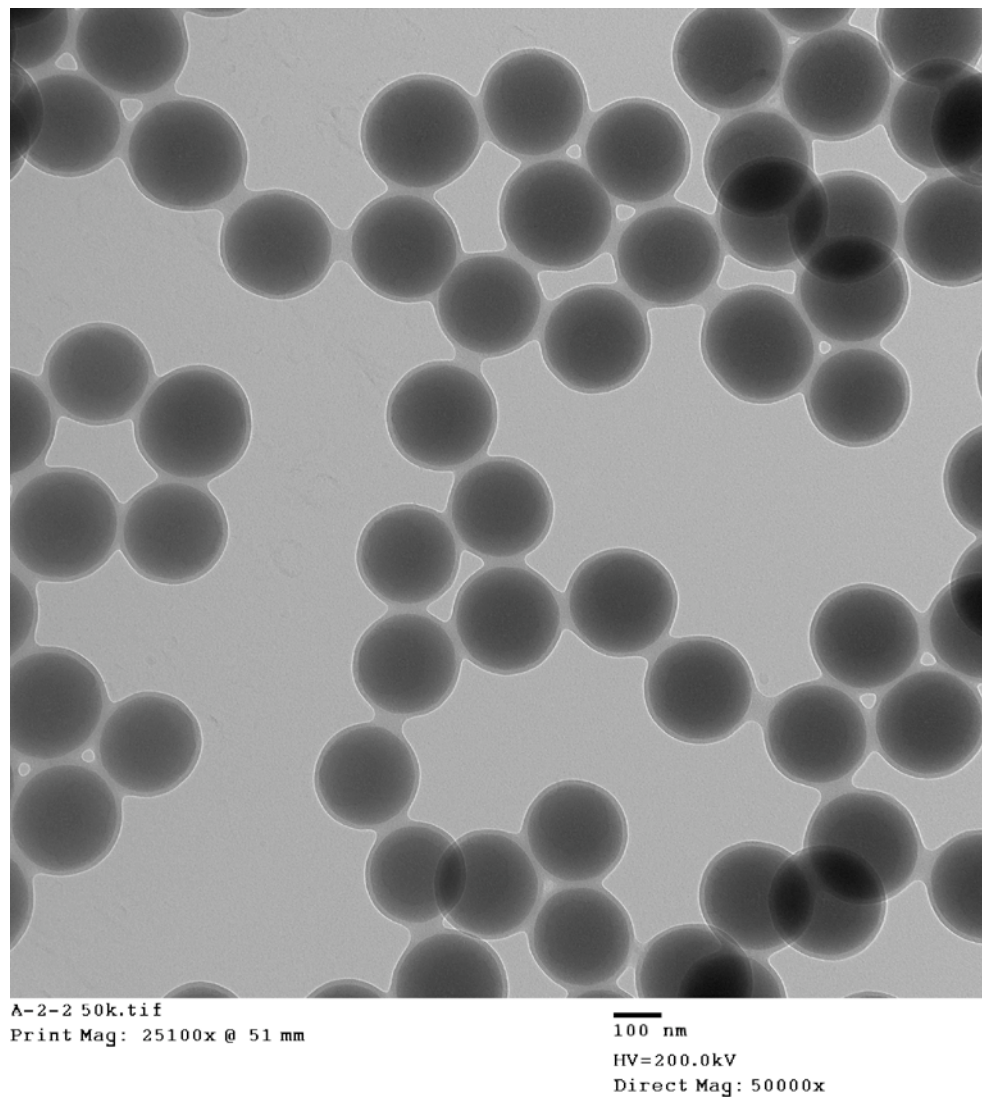


Figure S12. TEM image of PNIPA-SiP using 207 nm silica particles modified with PNIPA of $M_n = 25,500$, and $M_w/M_n = 1.29$.

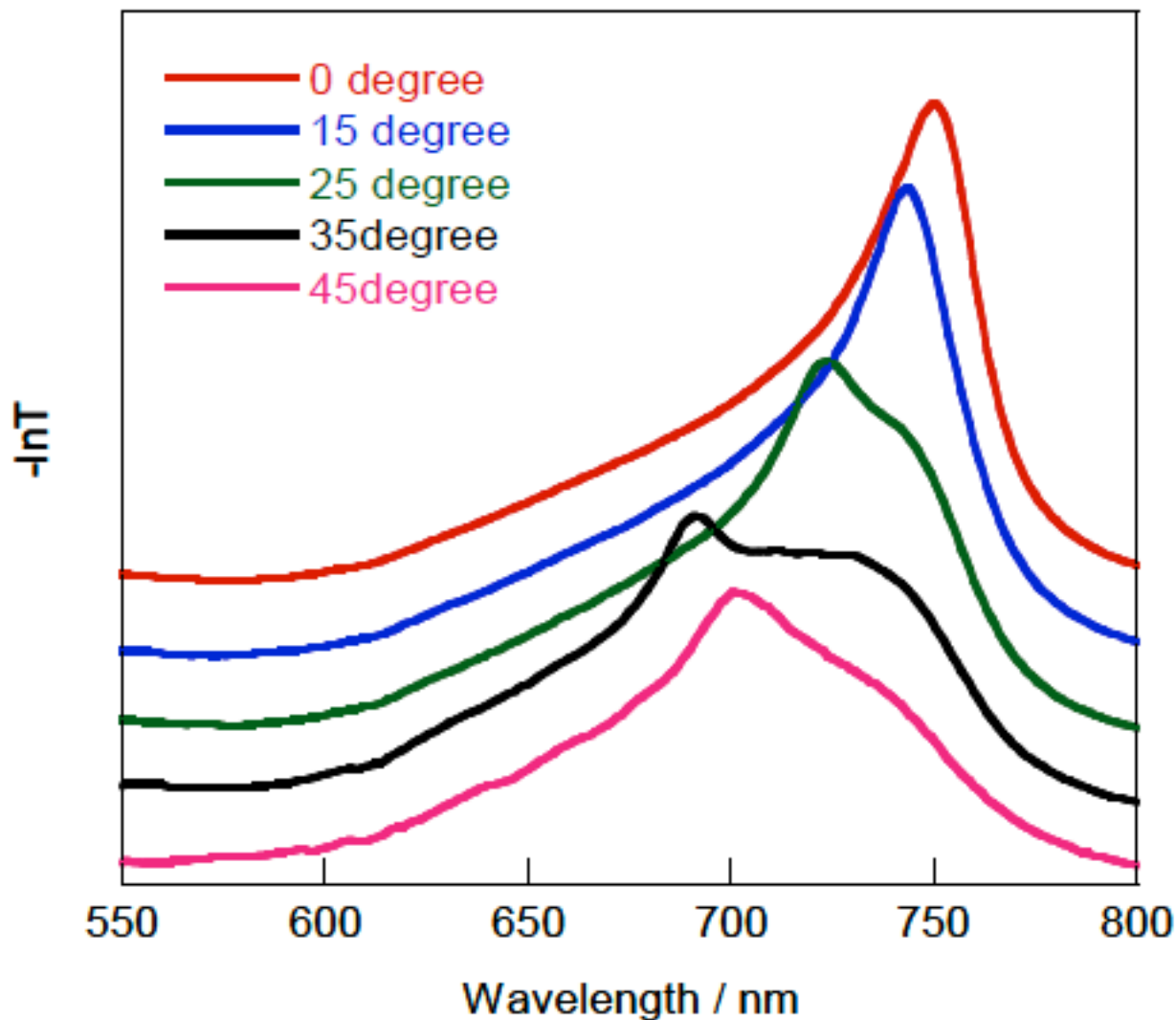


Figure S13. Transmission spectra of the thin membrane of colloidal crystal composed of PNIPA-SiP with 207 nm silica core particle and PNIPA of $M_n = 2.55 \times 10^4$ measured at various angles at 25° C. This thin membrane was prepared from the ethanol suspension of the PNIPA-SiPs.

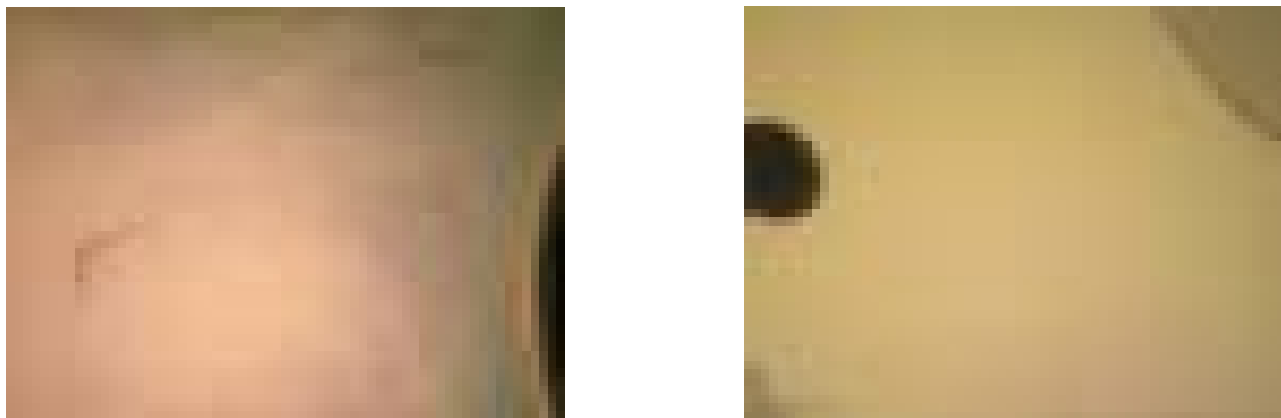


Figure S14. Photographs of the thin membrane of colloidal crystal (left) and the amorphous array (right) composed of PNIPA-SiP with 207 nm silica core particle and PNIPA of $M_n = 2.55 \times 10^4$ measured at various angles at 25° C. Both of them are opaque due to the multiple scattering of light from the presence of disordered portions.